Mars Perihelion Cloud Trails as revealed by MARCI: Mesoscale Topographically Focused Updrafts and Gravity Wave Forcing of High Altitude Clouds

R. T. Clancy, **M. J. Wolff**, **N. G. Heavens**, **P. B. James**, **S. W. Lee**, **B. J. Sandor,** *Space Science Institute, Boulder, CO USA (clancy@spacescience.org),* **B. A. Cantor, M. C. Malin,** *Malin Space Science Systems, San Diego, CA USA,* **D. Tyler, Jr.**, *Oregon State University, Corvallis, OR USA, and* **A. Spiga,** *LMD/IPS, Sorbonne University, Paris FR.*

Published in Clancy et al., Icarus, **362**, 2021.

Introduction:

The study of high altitude Mars clouds is stimulated by the wide variety of properties and behaviors of mesospheric (z > 50km) aerosols (e.g., Clancy et al., 2019). Mars mesospheric aerosols reflect distinctive processes such as large-scale dust storm injection of dust (e.g., Kleinböhl et al, 2019), saturation/condensation of the bulk atmosphere (i.e., CO_2; e.g., Listowski et al., 2014), and gravity-wave generation of discrete ice clouds (CO_2 and H_2O; e.g., Spiga et al., 2012). Here, we employ MARCI wide angle global imaging (Malin et al, 2008) to reveal another class of Mars water ice clouds at the base of the mesosphere (40-50 km), with distinctive EW linear morphologies and mesoscale, plume-like formation regions tied to southern perihelion topographic updrafts. These mesoscale updrafts generate vigorous gravity wave forcing, which leads to cloud formation 30-40 km above these topographic convergence updrafts, where the cloud ice particles are then rapidly transported westward in the rapid zonal circulation of the lower mesosphere.

Figure 1: MARCI color image projection of perihelion cloud trails (PCT) in association with Valles Marineris (from Clancy et al, 2009).

Daily, global imaging of Mars clouds in MARCI (MARs Color Imager, Malin et al., 2008) ultraviolet and visible bands yields the spatial/seasonal distributions and physical characteristics of perihelion cloud trails (PCT). PCT are a class of high altitude (40-50 km), horizontally extended (200-1000 km) water ice clouds that are aligned with the W to WSW

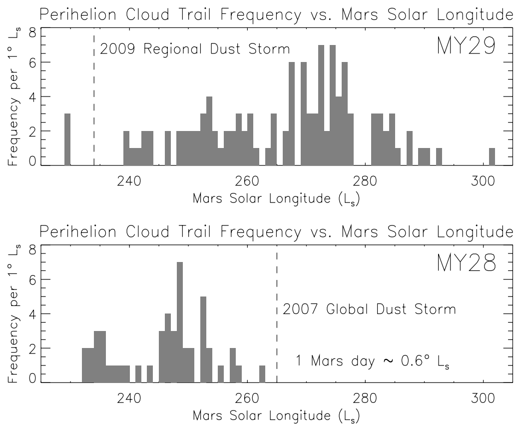

Figure 2: The global occurrence frequency of PCT in MY 28 (lower, global dust storm) and MY29 (upper, regional dust storm). Enhanced dust solar heating during dust storm activity suppresses water vapor saturation at the 40-50km altitudes of PCT formation.

direction of strong winds associated with the low-to-mid latitude lower mesosphere during Mars southern summer. The eastern cloud-forming mesoscale (N-S scales ~50 km) origins of PCT appear over specific southern low-to-mid latitude (5S-40S) locations in association with significant topographic gradients.

Such mesoscale cloud trails were first reported in association with northern and southern rim regions of Valles Marineris (figure 1, Clancy et al., 2009). The

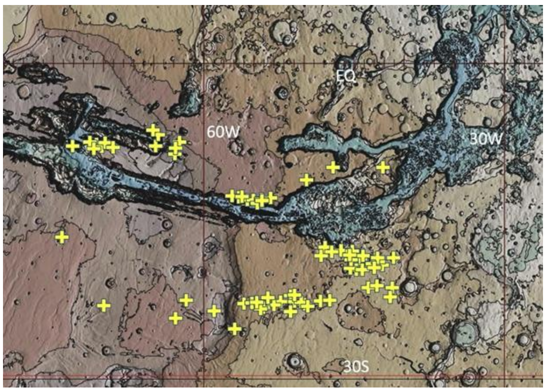

Figure 3: PCT eastern margin (formation regions) identified in MARCI 2007-2011 imaging in the Valles Marineris region (on USGS topography map). The wider range of PCT occurrence appear in figure

current study employs MARCI 2007-2011 imaging of PCT; and indicates several distinct locations of PCT occurrences (figure 7), including S W Arsia Mons, elevated regions of Syria, Solis, and Thaumasia Planitia, along Valles Marineris margins (figure 3), and the NE rim of Hellas Basin. PCT appear daily on a global basis (but not at a single location, figure 2) over Mars solar longitudes (L_s) of 210-310º, in late morning to mid-afternoon hours (10am-3pm), they are among the brightest and most distinctive clouds exhibited during the perihelion portion of the Mars orbit. Their locations (i.e., eastern margin origins) correspond to strong local elevation gradients, and their timing to peak solar heating conditions (perihelion, subsolar latitudes and midday local times). Based on cloud surface shadow analyses, PCT form at 40-50 km aeroid altitudes, where water vapor is generally at near-saturation conditions in this perihelion period (e.g. Millour et al., 2014). PCT were notable absent during periods of planet encircling and regional dust storm activity in 2007 and 2009, respectively, presumably due to reduced water saturation conditions above 35-40 km altitudes associated with increased dust heating over the vertically extended atmosphere (e.g., Neary et al., 2019).

PCT exhibit smaller particle sizes (R_{eff} = 0.2-0.5μm, 0.5μm, figure 4) than are typical in the lower atmosphere, but quite are optically bright ($\tau_{vis} \sim 0.1$) as they incorporate significant fractions (20-50%) of the available water vapor at these altitudes.

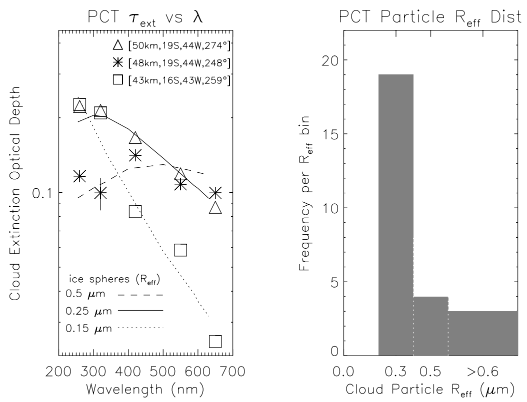

Figure 4: PCT Ice particle sizes from MARCI uv-vis imaging of cloud surface shadow extinctions.

PCT ice particles are inferred to form continuously (over ~4 hours, figure 5) at their PCT eastern origins, associated with localized updrafts, and are entrained in upper level zonal/meridional winds (towards W or WSW with ~50 m/sec speeds at 40-50 km altitudes) to create long, linear cloud trails.

PCT cloud formation is apparently forced in the lower atmosphere (≤10-15 km) by strong updrafts associated with distinctive topographic gradients,

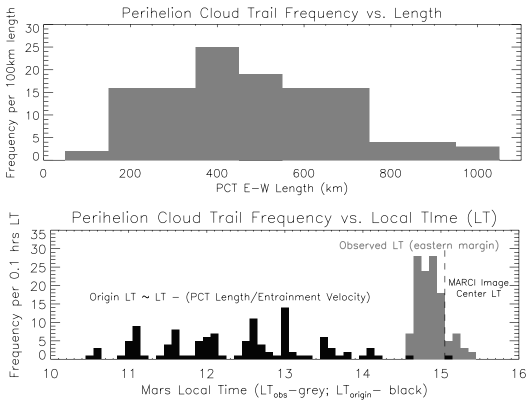

Figure 5: Observed lengths (upper) and local times of origin (bottom, grey) for PCT are limited by the MARCI fov in longitude and local time (LT). For a 50 m/sec growth in the PCT westward extension, MARCI length and eastern margin LT imply a wide range of daytime (10am-3pm, black) initiation LT.

such as simulated in mesoscale studies (e.g., Tyler and Barnes, 2015) and indicated by the surface specific PCT locations (figure 3, 7). These lower scale height updrafts are proposed to generate vertically propagating gravity waves (GW), leading to PCT formation above ~40 km altitudes where water vapor saturation conditions promote vigorous cloud ice formation (figure 6).

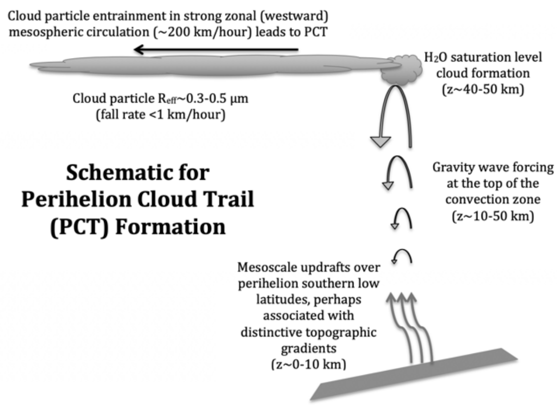

Figure 6: A schematic of PCT formation and evolution. The 4 key factors are topographic updrafts, gravity wave generation and propagation to 40-50 km region of near-saturation water vapor conditions, and resulting ice clouds entrained in westerly circulation.

Recent mapping of GW amplitudes at ~25 km altitudes, from Mars Climate Sounder 15 μm radiance variations (Heavens et al., 2020), in fact demonstrates close correspondences to the detailed spatial distributions of observed PCT (figure 7), relative to other potential factors such as surface albedo and surface elevation (or related boundary layer depths).

We note that a one-to-one correspondence in GW amplitudes at ~25 km and PCT at 40-50km is not expected, given spatial variations in GW propagation to >40 km and saturation conditions at 40-50km that lead to PCT formation. The implied correspondence of PCT (and MCS GW amplitudes at ~25 km) to topographic updrafts suggests such updrafts are a potentially significant mesoscale contribution to GW forcing in the current Mars atmosphere.

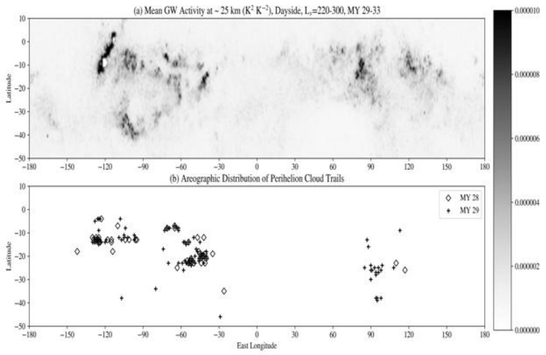

Figure 7: Apparent spatial correspondence of MCS-derived gravity wave amplitudes at ~25 km (Heavens et al., 2020; upper panel) to the spatial distribution of PCT at 40-50 km from MARCI imaging (Clancy et al. 2021).

References:

Clancy, R.T., Wolff, M.J., Cantor, B.A., Malin, M.C., Michaels, T.I., 2009. Valles Marineris cloud trails, *J. Geophys. Res.* **114** (E13), 11002.

Clancy, R.T., Wolff, M.J., Smith, M.D., Kleinböhl, A., Cantor, B.A., Murchie, S.L., Toigo, A.D., Seelos, K., Lefèvre, F., Montmessin, F., Daerden, F., Sandor, B.J., 2019. The distribution, composition, and particle properties of mars mesospheric aerosols: An analysis of CRISM visible/near-IR limb spectra with context from near- coincident MCS and MARCI observations. *Icarus* **328**, 246–273.

Clancy, R.T., Wolff, M.J., Heavens, N.G., James, P.B., Lee, S.W., Sandor, B.J., Cantor, B.A., Malin, M.C., Tyler Jr, D., Spiga, A., 2021. Mars perihelion cloud trails as revealed by MARCI: Mesoscale topographically focused updrafts and gravity wave forcing of high altitude clouds, *Icarus* **362**, 114411.

Heavens, N.G., Kass, D.M., Kleinböhl, A., Schofield, J.T., 2020. A multiannual record of gravity wave activity in Mars' lower atmosphere from on-planet observations by the Mars Climate Sounder, *Icarus* **341**, 113630.

Kleinböhl,A., Spiga, A., Kass, D.M., Shirley, J.H., Millour, E., Montrabone, L., Forget, F., 2019. Diurnal variations of dust during the 2018 global dust storm observed by the Mars Climate Sounder, 2019. *J. Geophys. Res*. **125**, e2019JE006115.

Listowski, C., Määttänen, A., Montmessin, F., Spiga, A., Lefèvre, F., 2014. Modeling the microphysics of CO_2 ice clouds within wave-induced cold pockets in the martian mesosphere. *Icarus* **237**, 239–261.

Malin, M.C., Calvin, W.M., Cantor, B.A., Clancy, R.T., Haberle, R.M., James, P.B., Thomas, P.C., Wolff, M.J., Bell, J.F., Lee, S.W., 2008. Climate, weather, and north polar observations from the Mars Reconnaissance Orbiter Mars Color Imager, *Icarus* **194**, 501–512.

Millour, E., Forget, F., Spiga, A., Navarro, T., Madeleine, J.-B., Montabone, L., Lefèvre, F., Chaufray, J.-Y., Lopez-Valverde, M.A., Gonzalez-Galindo, F., Lewis, S.R., Read, P.L., Desjean, M.-C., Huot, J.-P., MCD/GCM Development Team, 2014. The mars climate database (MCD version 5.1). LPI Contrib. 1791, 1184.

Neary, L., Daerden, F., Aoki, S., Whiteway, J., Clancy, R.T., Smith, M., Viscardy, S., Erwin, J.T., Thomas, I.R., Villanueva, G., Liuzzi, G., Crismani, M., Wolff, M., Lewis, S.R., Holmes, J.A., Patel, M.R., Giuranna, M., Depiesse, C., Piccialli, A., Robert, S., Trompet, L., Willame, Y., Ristic, B., Vandaele, A.C., 2019. Explanation for the increase in high-altitude water on mars observed by NOMAD during the 2018 global dust storm, *Geophys. Res. Lett.* **47** (7), e84354.

Spiga, A., González-Galindo, F., López-Valverde, M.-Á., Forget, F., 2012. Gravity waves, cold pockets and CO_2 clouds in the martian mesosphere. *Geophys. Res. Lett.* **39**, L02201.

Tyler, D., Barnes, J.R., 2015. Convergent crater circulations on mars: Influence on the surface pressure cycle and the depth of the convective boundary layer. *Geophys. Res. Lett*. **42**, 7343–7350.